V. Anil Kumar, R. K Gupta*, Vinod Kumar and P. V Venkitakrishnan

Effect of Prior Thermomechanical Treatment on Annealed Microstructure and Microhardness in Cobalt-Based Superalloy Co-20Cr-15W-10Ni

DOI 10.1515/htmp-2016-0158
Received July 17, 2016; accepted January 28, 2017

Abstract: Microstructure evolution in Co-20Cr-15W-10Ni alloy with hot deformation and subsequent annealing has been studied using hot isothermal compression at different temperatures and strain rates followed by annealing at 1,423 K for 1 h. In the as-deformed condition, optical microstructure reveals deformation bands in specimens deformed at low temperature (1,323 K) and high strain rate (10 s^{-1}). In deformation beyond 1,423 K, very fine recrystallized grains are observed at all the strain rates, which is seen to be fully developed at 1,473 K onwards especially at lower strain rates (0.1 and 0.01 s^{-1}). EBSD maps reveal recrystallized grains and presence of deformation twins. Grain growth is observed at strain rate lower than 0.1 s^{-1} and temperature more than 1,473 K. After annealing of deformed samples, fully recrystallized grains and annealing twins have been observed. Samples subjected to prior deformation at higher strain rates showed mixed grains with small banding of recrystallized structure, whereas more uniform recrystallized microstructure is observed at slow strain rates. Microhardness decreases with increase in deformation temperature. However, annealed hardness is found to be increasing marginally with decreasing prior deformation temperature (especially for slower strain rates), attributing to relatively uniform and fine microstructure after annealing.

Keywords: cobalt based superalloy, microstructure, annealing

***Corresponding author: R. K Gupta,** Materials and Mechanical Entity, Vikram Sarabhai Space Centre, ISRO, Trivandrum, India, E-mail: rohitkumar_gupta@vssc.gov.in
V. Anil Kumar, Materials and Mechanical Entity, Vikram Sarabhai Space Centre, ISRO, Trivandrum, India
Vinod Kumar, Steel Authority of India Ltd., RDCIS, Ranchi, India
P. V Venkitakrishnan, Mechanical engineering entity, Vikram Sarabhai Space Centre, ISRO, Trivandrum, India, E-mail: venkitakrishnanpv@gmail.com

Introduction

Cobalt-based superalloy Co-20Cr-15W-10Ni is extensively used for medical, aerospace and power sectors not only due to high temperature properties but also due to good corrosion resistance. Being a single phase alloy, its workability is good, however process control is required to obtain desired microstructure for further processing and application. It has been reported to be superior to nickel-based superalloys due to better resistance to thermal shocks and hot gas corrosion [1]. Like other superalloys, the microstructure consists of face centered cubic (FCC) γ-matrix with some strengthening phases. However, the precipitation hardening does not play role in this alloy. Finally, strength of the alloy depends on solid solution strengthening and carbide formation [1–3].

Hot working temperature of this alloy lies in the temperature range of 1,373 K–1,523 K. But to control the grain size and achieve desired mechanical properties, lower finishing temperature along with higher reduction is required. Also response to annealing after forging is influenced by these parameters, which finally decides the grain size of the alloy. Being essentially a single phase alloy, grain size plays important role in fabrication as well as in service.

Microstructure evolution during forging and subsequent annealing has been reported [4]. The alloy forms annealing twins during annealing. Martensite phase formation has not been reported with any particular heat treatment, however, stress-induced martensitic transformation (SIMT) is possible during plastic deformation at lower temperature [2]. Formation of intermetallic phases and carbides is expected at 873–1,373 K only after prolonged exposure [5, 6]. It has also been reported that carbide precipitation does not take place during annealing heat treatment for a duration less than 1 hour at any temperature. Further, to avoid Laves phase formation and minimize carbide phases without grain coarsening, desired annealing temperature is selected [4]. Mainly M_6C and $M_{23}C_6$ type carbides have been reported in this alloy [2, 3, 7]. Laves phase (Co_2W), which is brittle is associated with formation of M_6C as platelet at grain

boundaries [8]. Considering all these factors, annealing temperature (>1,373 K) and time (<1 h) are selected.

Several studies have been made to study the intermetallics/carbides, effect of long exposure at high temperatures, hot deformation etc., but study focusing on microstructure evolution and static recrystallization during hot deformation at wide regime of temperature/strain rates is limited. Hot compression test was carried out and deformation behavior has been reported elsewhere [5, 9]. Further, microstructure evolution in as compressed samples and after annealing is important to optimize the deformation processing so that desirable microstructure can be obtained after annealing. A systematic study on evolution of microstructure in hot deformation through isothermal compression (under varying temperatures and strain rates) and static annealing at a constant temperature and time is presented here. Thorough microstructural analysis has been carried out using optical microscopy (OM) and electron back scatter diffraction (EBSD) methods. Microhardness of as-hot deformed samples as well as after static annealing has also been correlated with microstructure and corresponding processing conditions.

Experimental details

Samples were taken from the forged billet made through vacuum induction melting (VIM) followed by electro-slag refining (ESR). Chemical composition of alloy is given in Table 1. Cylindrical samples of dia. 10 mm × 15 mm height were machined by wire EDM from the forging for carrying out hot isothermal compression studies at different temperatures in the range of 1,323–1,523 K at 50 K intervals and at strain rates of 10^{-2}, 10^{-1}, 10^{0} and 10^{1} s^{-1}. Gleeble thermo-mechanical simulator has been used for hot compression. For measuring the temperature of the specimen during deformation, a thermocouple is welded to the surface of the specimen and temperature is recorded. The samples were heated to the deformation temperature at the rate of 5 Ks^{-1} and then held at the deformation temperature for 60 s before applying load. The deformed specimens were then cooled/quenched to room temperature in water. Cross section of the deformed specimens were cut through wire EDM and prepared for microstructure observation. Further, annealing has been carried out at 1,423 K for 1 h. Optical microscopy, electron back scatter diffraction (EBSD) and microhardness survey been conducted on as compressed samples and compressed plus static annealed samples.

Specimen preparation for optical microscopy was carried out through conventional mechanical polishing technique. Polished specimens were etched with 4 % H_2SO_4 by electrolytic etching technique. Microstructure was observed under Olympus make optical microscope.

Samples for EBSD were prepared by conventional metallographic polishing followed by fine colloidal silica polishing. The samples were then subjected to electro-polishing using 80 % methanol, 20 % perchloric acid mixture at a temperature of 273 K and voltage of 16 V for 30 s in Struers-make Lectropol-5 model electropolishing machine. EBSD was done in FEI make Quanta 30 KV 3D FEG-SEM. EBSD maps were recorded on a scan area of 500 × 1,000 μm and step size of 1 μm. The EBSD data thus obtained was analyzed using TSL OIM software. Wilson make Vickers micro-hardness tester was used to determine the microhardness of the specimen using a load of 300 gf for 10 s.

Results and discussion

In general, hot compression of this superalloy is found to be good and compressed specimen does not show any signature of crack/defect formation except thin oxide scale over the surface at outer periphery. This also indicates that material has good workability in the range of 1,523 to 1,323 K under the strain rates of 0.01 to 10 s^{-1}.

Microstructure

Optical microstructure of initial condition of the parent metal is presented in Figure 1. Palettes of microstructures of vertical cross section of the specimens subjected to hot isothermal compression and compressed plus annealed are presented in Figures 2 and 3 respectively. The alloy

Table 1: Chemical composition of Cobalt based superalloy.

Elements	C (max.)	Cr	W	Ni	Fe (max.)	Mn	Si (max)	Co
Specified, wt%	0.15	19–21	14–16	9–11	3	1–2	0.40	Bal.
Actual, wt%	0.080	19.95	14.16	10.82	0.10	1.35	0.09	

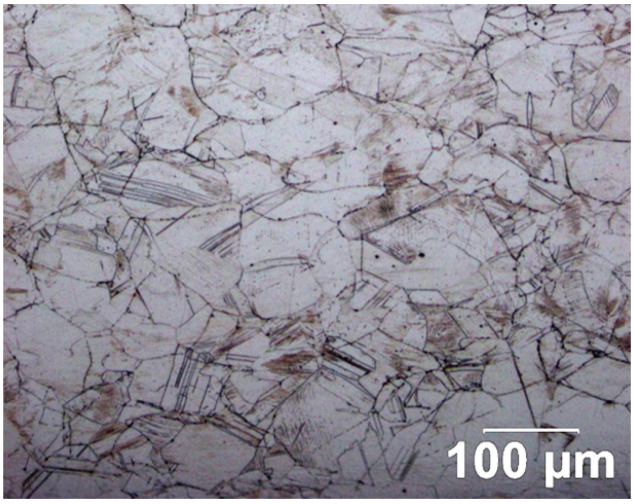

Figure 1: Optical microstructure of forged + annealed sample (initial condition).

mainly contains cobalt rich austenitic grains with $M_{23}C_6$ and M_6C as primary carbides [4, 5]. Hot deformed specimen cross section shows variety of microstructures (Figure 2). At 1,323 K, microstructure shows flow of grains perpendicular to the applied stress and presence of fine recrystallized grains at the intergranular sites. This indicates initiation of nucleation for recrystallization, which is very fine at higher strain rates (10 s^{-1}, Figure 2 top left corner) and increases in size with decrease in strain rates (Figure 2 bottom left corner). This phenomenon can be seen almost in all the specimens but to a different degree and as the temperature rises, disappearance of deformed grains and appearance of only dynamically recrystallized grains are seen for the same strain rate. At sufficiently higher temperatures, effect of recrystallization is totally eliminating the signature of deformed structure and at 1,423 K recrystallized structure (third column from left of Figure 2 top to bottom) is formed even at high strain rates to low strain rates, showing marginal higher size of recrystallized grains toward lowering in strain rates. Further, at 1,473 K and 1,523 K microstructure is fully recrystallized structure at all the strain rates, where increase in size of recrystallized grains is clearly visible (4^{th} and 5^{th} column from left, Figure 2, top to bottom). Growth of recrystallized grains with decreasing strain rate is due to availability of time.

Also, indication of fine adiabatic shear band formations is observed in samples tested at temperature of 1,323 K and strain rate of 10 s^{-1} (Figure 2). This indicates the initiation of recrystallized grains between the shear bands which propagates throughout the material with change in temperature and strain rates and finally develops into recrystallized grains throughout the material.

The deformed specimens, when subjected to annealing behave (Figure 3) according to microstructural variation as noted prior to annealing (Figure 2). It can be clearly seen that degree of recrystallization is varying

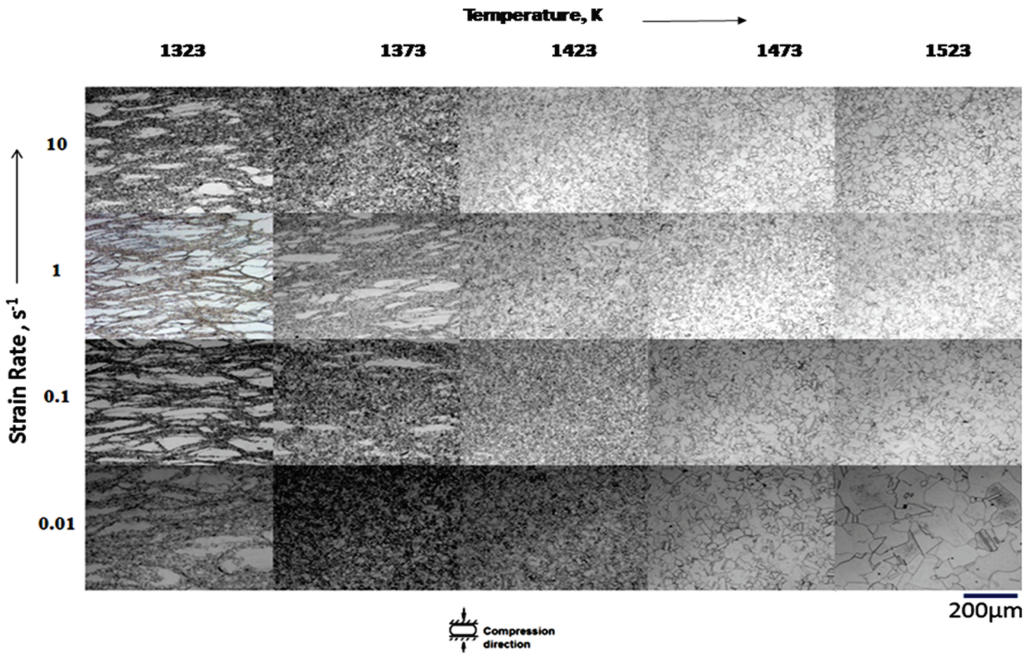

Figure 2: Optical microstructures of specimens deformed at different conditions.

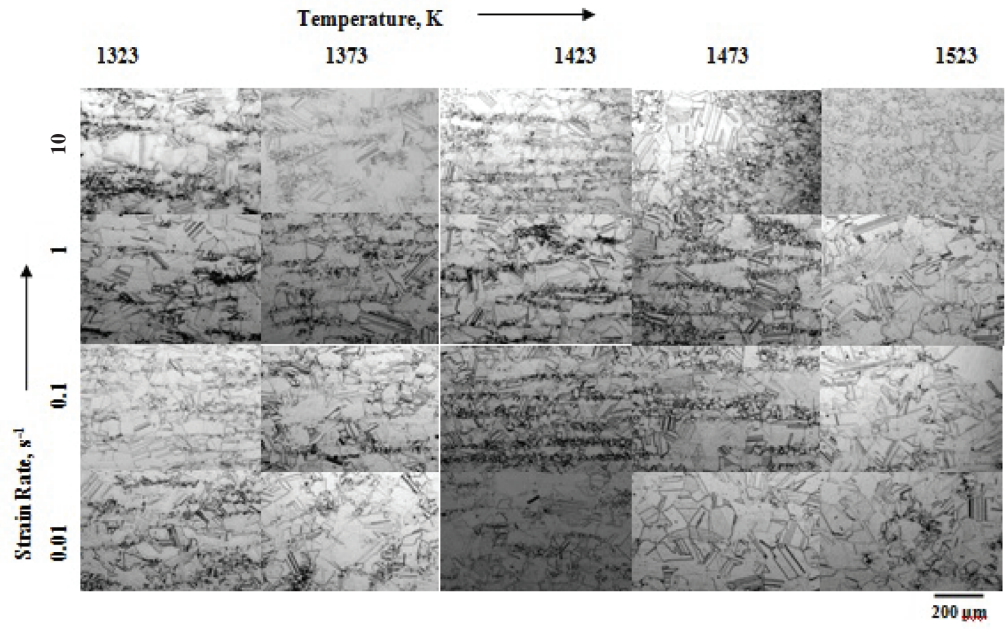

Figure 3: Optical microstructures of the static annealed specimens prior deformed at different conditions.

due to the variation in stored energy due to prior deformation. Specimens deformed at lower temperature and higher strain rates (top left corner, Figure 3) consist of non-uniformly recrystallized grains. It is due to large amount of deformation bands and presence of fine nuclei during deformation, which grow during annealing differentially. Already recrystallized grains become coarse and fine nuclei develop into fine recrystallized grains. The same situation continues for higher temperature deformed grains and with decrease in strain rates. It is the amount of energy provided to the deformed samples, which intrinsically consist of different degree of recrystallization/deformation bands and amount of residual stresses. From Figure 3, it can be seen that at the strain rate of 10 s^{-1}, as the temperature increases mostly fine uniform microstructure develops and similarly at lower strain rates (where sufficient time is available) microstructure becomes mostly uniform with increase in temperature (but coarser as compared to former case). At intermediate strain rates 0.1 and 1, recrystallized grains are seen in the form of bands especially at lower temperatures, which disappears at 1,523 K and develop grains of uniform size.

Another important observation for the present alloy is the formation of twins. Forged and annealed sample (Figure 1) shows presence of twins. This original structure when compressed at different temperature and strain rate conditions does not reveal clearly the presence of twins (Figure 2). Only few sample show fully developed twins in as compressed condition (Figure 2 right bottom corner) where temperature is sufficiently high and strain rate is low. This indicates twinning is another important deformation mechanism for this alloy. Though alloy consists of fcc matrix at high temperature, but still deformation is assisted by twinning when deformation is restricted by other mode (slip). As the required amount of energy is not available (at low temperature and high strain rate) only deformation bands are observed. However at higher temperature and slower strain rates, deformation twins develop with the available energy. This phenomenon continues and as soon as compressed specimens are subjected to annealing treatment new strain free twins (annealing) are formed, which also show a trend similar to formation of recrystallized grains (according to prior compression temperature and strain rates). Higher amount of twins and with wider twin boundaries can be clearly seen for higher temperature and slower strain rates deformed samples after annealing treatment (Figure 3), which is due to similar reasons as explained for recrystallized grains.

Dynamic recrystallization is the predominant mechanism in hot deformation in the alloy and dynamic recovery may also be operative along with dynamic recrystallization at lower temperatures. Dynamic recrystallization helps in

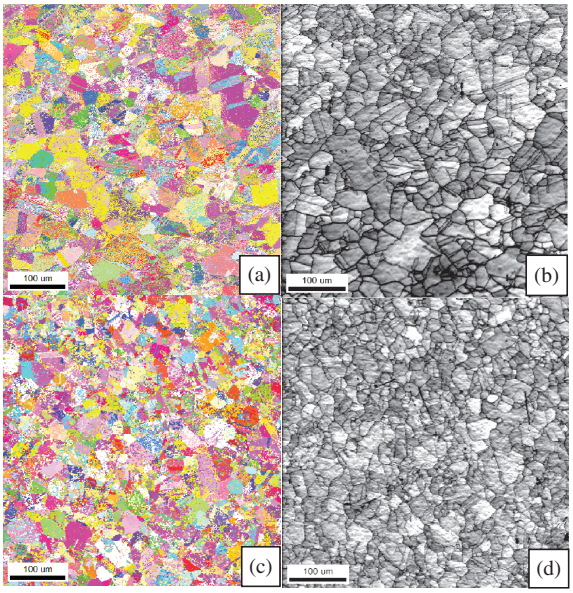

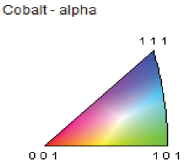

Figure 4: Inverse pole figure maps (a, c) and image quality maps (b, d) in (a, b) 1,473 K/0.01 s^{-1} (c, d) 1,473 K/0.1 s^{-1}.

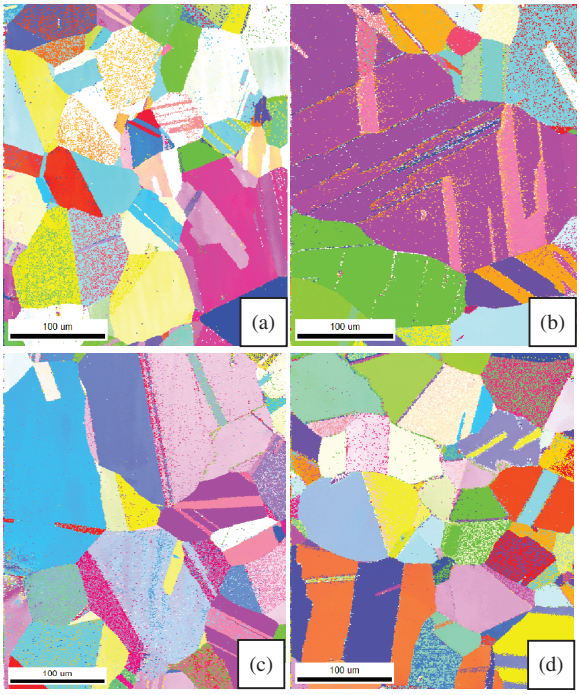

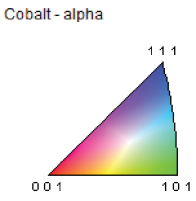

Figure 5: Inverse pole figure maps of annealed specimens after compression (at different temperature and strain rates) (a) 1,323 K/0.1 s^{-1} (b) 1,473 K/0.01 s^{-1} (c) 1,473 K/0.1 s^{-1} (d) 1,523 K/0.1 s^{-1}.

flow softening during hot deformation at higher temperatures, which is prevalent in this alloy due to low stacking fault energy (SFE) and poor mobility of the dislocations [8].

Further, EBSD maps presented in Figures 4 and 5 also substantiate the observations made through optical microscopy along with additional information on microtexture. Representative inverse pole figure (IPF) maps and respective image quality maps of the alloy in hot isothermal compressed conditions at 1,473 K temperature and 0.01 s^{-1}, 0.1 s^{-1} strain rates is shown in Figure 4. They clearly show presence of very fine recrystallized grains with random textures and image quality maps show deformation twins (Figure 4(b) and 4(d)). At all other temperatures and strain rates, EBSD

maps reveal variation in degree of recrystallization, random textures and presence of deformation bands (mainly at low temperature and high strain rate compressed specimens) and twins (in almost all the compressed samples). Recrystallized grain size (20–130 μm) increases with increasing temperature and decreasing strain rates.

Formation of necklace/banding of fine grains as seen in optical photomicrographs (Figures 2 and 3) is also seen in the EBSD maps. It means microstructures contain grains of non-uniform size. After annealing of the compressed samples, generation of large amount of annealing twins has been observed (Figures 5 and 6). Being low stacking fault energy material, twinning is also an important mode of deformation (deformation twins) and restoration (annealing twins). There is no significant change in texture/orientation after annealing, but coarsening of grains and development of twins are clearly seen in all the samples. This indicates formation of annealing twins is the major factor in restoration process. After annealing, IPF maps and IQ maps clearly confirm that effect of low temperature with moderate strain rate (0.01 s^{-1}) compression is better with respect to attaining nearly uniform microstructures.

Microhardness

Microhardness survey of compression tested specimens and annealed specimens was carried out and is presented in Figure 7. It can be seen from Figure 7(a) that microhardness increases from 239 Hv to 383 Hv with decreasing temperatures (from 1,523 K to 1,273 K). Similar increasing trend in microhardness is noted with increasing strain rates, except in the case of high strain rates of 10 s^{-1}. Marginal lower microhardness at 10 s^{-1} as compared to 1 s^{-1} may be due to flow softening due to additional adiabatic heating (possible at higher strain rates).

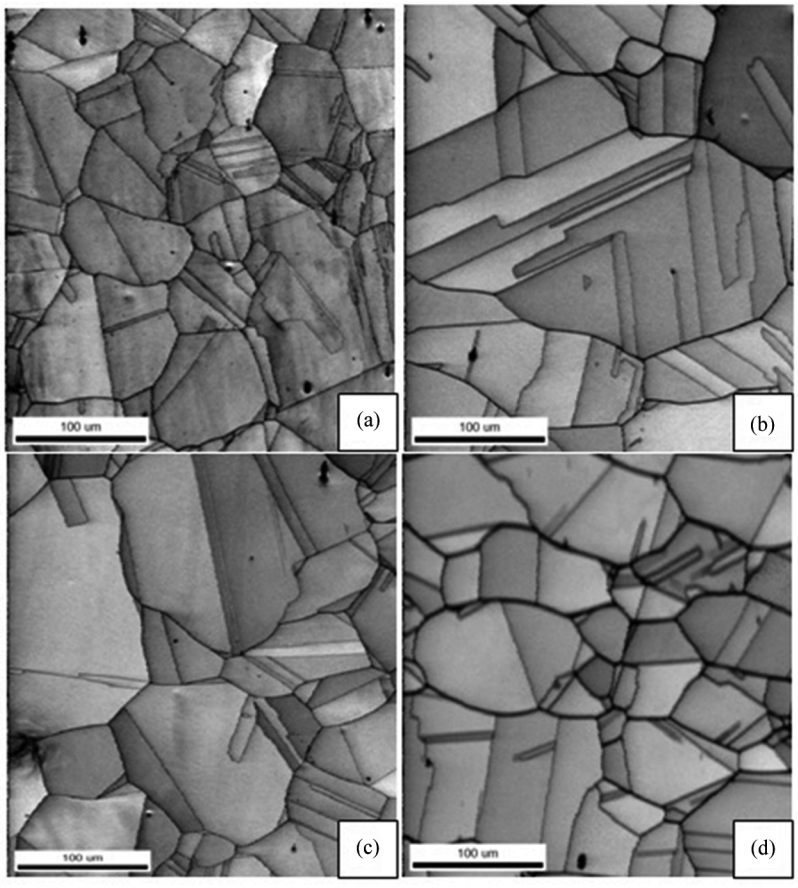

Figure 6: Image quality maps of annealed specimens after compression (at different temperature and strain rates) (a) 1,323 K/0.1 s^{-1} (b) 1,473 K/0.01 s^{-1} (c) 1,473 K/0.1 s^{-1} (d) 1,523 K/0.1 s^{-1}.

Microhardness measurement after annealing as shown in Figure 7(b) shows small variation from the as hot compressed samples. Sample compressed at lower strain rates is found to have moderately uniform microhardness for change in temperature from 1,323 to 1,523 K. However, this trend is not noted for sample compressed at higher strain rates. It shows material deformed at higher strain rate still follows the trend of as compressed samples especially at 10 and 1 s^{-1} strain rates. Microhardness of as compressed sample is found to be in the range of 270 to 383 Hv, whereas it is only 253 to 315 Hv after annealing indicating more closer range, i. e. improvement in uniformity.

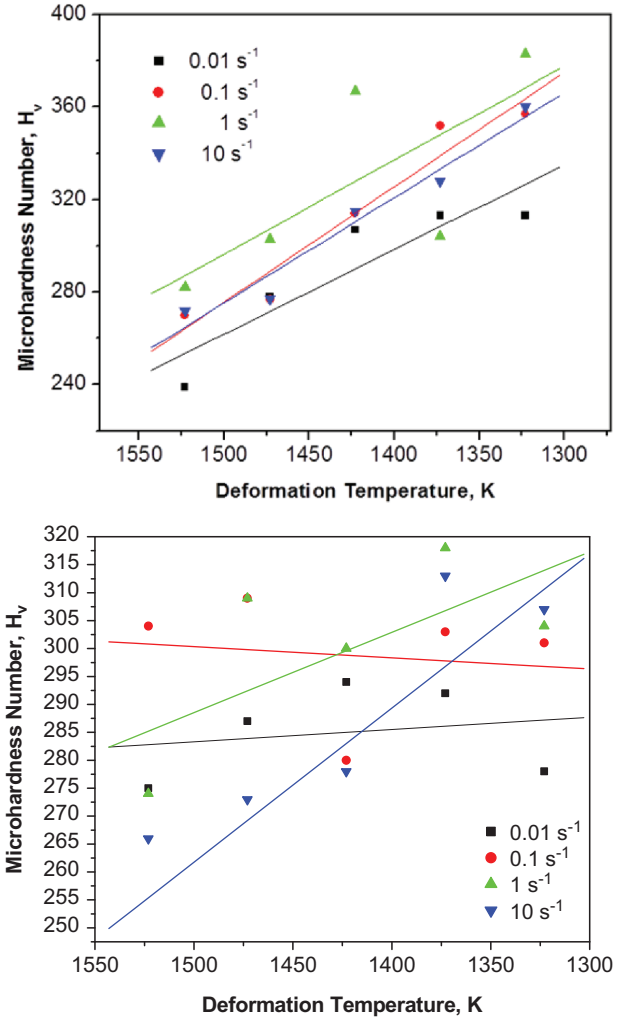

Figure 7: Variation of microhardness with temperature and strain rate, (a) As hot compressed, (b) hot compressed and annealed.

Conclusions

Hot isothermal compression of Co-Cr-W-Ni alloy is carried out at temperature ranging from 1,323 K–1,523 K and with strain rate of 0.01 to 10 s^{-1} and subsequent annealing is carried out at 1,423 K for 1 h. Following conclusions are derived from the study.

1. Microstructures are found to be consisting of refined DRX grains after hot isothermal deformation. Electron back scatter diffraction (EBSD) image clearly shows presence of twins indicating their assistance in deformation.
2. Growth of dynamically recrystallized grains is observed with increasing temperature and decreasing strain rate and vice versa. Formation of DRX grains at 1,323 K indicates that it is the minimum temperature of deformation to trigger recrystallization.
3. Almost all samples subjected to static annealing revealed presence of annealing twins which may have nucleated from the prior recrystallization nuclei formed during deformation.
4. Microhardness of as compressed sample is found to be in the range of 270 to 383 Hv, whereas it is only 253 to 315 Hv after annealing indicating uniformity.

Acknowledgments: The authors are thankful to GM, MMA and DD, MME for the encouragement and support provided during this work. The authors are also thankful to Director, VSSC for granting permission to publish this work.

References

[1] B. Geddes, H. Leon and X. Huang, Superalloys: Alloying and Performance, ASM Handbook (2010).
[2] B.S. Lee, H. Matsumoto and A. Chiba, Mater. Lett., 65 (2011) 843–846.
[3] N. Yukawa and K. Sato, Trans. Japan Inst. of Metals, 9 (1968) 680–686.
[4] R.K. Gupta, M.K. Karthikeyan, D.N. Bhatia, B.R. Ghosh and P.P. Sinha, Metal Sci. and Heat Treat., 50 (2008) 175–179.
[5] Y. Julien Favre, K.A. Chiba, D. Fabregue and E. Maire, Metall. and Mater. Trans., 44A (2013) 2819–2829.
[6] R.B. Herchenvoeder and W.T. Ebihara, Metals Eng. Quart., (1969) 313–324.
[7] S.T. Wlodek, Trans. ASM, 56 (1963) 287–303.
[8] J. Teague, E. Cerreta and M. Stout, Metall. and Mater. Trans., 35A (2004) 2767–2781.
[9] V. Anil Kumar, R.K. Gupta, S.V.S. Narayana Murty and A.D. Prasad, J. Alloys and Comp., 676 (2016) 527–541.